Positive Impulsive Control of Tumor Therapy—A Cyber-Medical Approach

Levente Kovács, *Senior Member, IEEE*, Tamás Ferenci, *Member, IEEE*, Balázs Gombos, András Füredi, Imre Rudas, *Life Fellow, IEEE*, Gergely Szakács, and Dániel András Drexler, *Member, IEEE*

Abstract—Chemotherapy optimization based on mathematical models is a promising direction of personalized medicine. Personalizing, thus optimizing treatments, may have multiple advantages, from fewer side effects to lower costs. However, personalization is a complicated process in practice. We discuss a mathematical model of tumor growth and therapy optimization algorithms that can be used to personalize therapies. The therapy generation is based on the concept of keeping the drug level over a specified value. A mixed-effect model is used for parametric identification, and the doses are calculated using a two-compartment model for drug pharmacokinetics, and a nonlinear pharmacodynamics and tumor dynamics model. We propose personalized therapy generation algorithms for having a maximal effect and minimal effective doses. We handle inter- and intra-patient variability for the minimal effective dose therapy. Results from mouse experiments for the personalized therapy are discussed and the algorithms are compared to a generic protocol based on overall survival. The experimental results show that the introduced algorithms significantly increased the overall survival of the mice, demonstrating that by control engineering methods an efficient modality of cancer therapy may be possible.

Index Terms—Impulsive system, min–max therapy, optimal treatment, positive system, therapy generation, tumor model.

I. INTRODUCTION

CYBER-MEDICAL systems play an important role in modern medicine, and their importance is growing. The application of STEM in medicine offers prosperous results in medical practice. For example, engineering methods can be used for brain fatigue detection [1], [2], [3], prediction of in-hospital death of trauma [4], skeleton maturity assessment [5], [6], or Parkinson's disease diagnosis [7]. System-theoretic methods are used in several drug dosing problems, like control of anesthesia [8], or control of blood glucose level with artificial pancreas [9].

System-theoretic methods can also be utilized to optimize drug dosing in cancer therapies. The therapies used in conventional chemotherapy usually have a large resting time, i.e., a long time between the injections and large injected doses [10]. They use the maximum tolerable dose (MTD) in order to achieve a maximal effect without killing the patient. Another approach is the low-dose metronomic (LDM) therapy, which applies lower doses with larger frequency. In some cases, this approach was proven more effective against cancer cells, which often become resistant to the treatment [11], [12]. LDM therapy can also be cheaper with fewer side effects. We aim to provide algorithms for the mathematical model-based generation of LDM therapies.

Scheduling LDM therapy and providing the required doses is a challenging task. A promising engineering approach is to use a mathematical model describing the effect of the drug on tumor growth and use this model to generate an optimal therapy. There are numerous models in the literature (see [10], [13], [14], [15] and several therapy generation algorithms [10], [16], [17], [18]). A specific characteristic of this physiological problem is that the input is the injection, which is positive, and the system is impulsive. Such systems are rare in engineering practice, and thus handling them requires unconventional solutions [19], [20], [21]. Besides therapy generation, the usage of nanorobots in cancer treatments is also exploited by Shi et al. [22], [23], [24], while robotic capsules are used for site-specific drug delivery in [25].

This article has been accepted for inclusion in a future issue of this journal. Content is final as presented, with the exception of pagination.

2

IEEE TRANSACTIONS ON SYSTEMS, MAN, AND CYBERNETICS: SYSTEMS

Pérez-García et al. [10] used their model and heuristic scheduling based on in silico tests. Tse et al. considered multidrug optimization problems in [26]. Cacace et al. [18] solved the therapy generation as an optimization problem to minimize a quadratic cost function combined with a state observer. They generate antiangiogenic therapy based on the model created by Hahnfeldt et al. [27]. The authors of this manuscript created an optimization algorithm for the antiangiogenic therapy based on the Hahnfeldt model in [16], where the aim was to track a reference path that results from maximal dosing with a predefined maximal deviation from that path. The authors used an approach based on pharmacokinetic (Section II-C) and pharmacodynamic (Section II-B) model to optimize chemotherapy in [17] and [28], based on the results of Kusuoka et al. [29]. Here, we develop the results further and provide several model-based approaches for the therapy generation problem.

The fundamental component of optimization is the underlying mathematical model. Our algorithm depends on the pharmacokinetics and pharmacodynamics of the drug; however, several strategies discussed here also depend on the tumor dynamics. The literature on tumor models is rich; see the works of [30], [31], and [32]; in our work, we use a tumor model described by ordinary differential equations.

We use a fourth-order model (Section II-A) created to describe measurements from animal experiments first for antiangiogenic therapy using bevacizumab [33], [34], and later for chemotherapy using pegylated liposomal doxorubicin (PLD) in [35] and [36] based on the experiments from [37]. The latest model has four state variables, two state variables to describe the living and dead tumor volume dynamics, and two state variables to describe the pharmacokinetics of the drug as a two-compartment model. We formulate the optimization problem as maintaining a predefined drug level during the therapy with the lowest amount of injections, i.e., we carry out optimal impulsive control of the two-compartment pharmacokinetic model and propose three strategies to calculate this predefined drug level.

Impulsive control of compartment systems is not new in the literature; e.g., the work of Pierce and Schumitzky from 1976 [38]. Kusuoka et al. [29] created an algorithm in 1981 for finding minimal doses that keep the drug level over a specified lower limit, discussed in Section II-D. Our work is based on this algorithm and contributes by defining the lower limit for the drug level, which we will call minimal inhibitory concentration (MIC) after [39] (see Fig. 1). We test the algorithms in vivo using mouse experiments discussed in Section IV-A.

We propose three strategies to define the lower limit of the drug level: two personalized therapies and one robust therapy created for a specific population. The first strategy is a personalized therapy aiming to maximize the effect of the drug using low dosages and only uses the pharmacokinetic and pharmacodynamic model (Section III-B). The second strategy is a personalized therapy, which finds the minimal effective dosages that ensure that the tumor volume does not increase during the therapy for constant and time-varying (but known) parameters (Section III-C). This strategy requires knowledge of the tumor dynamics as well. The third strategy is the robust
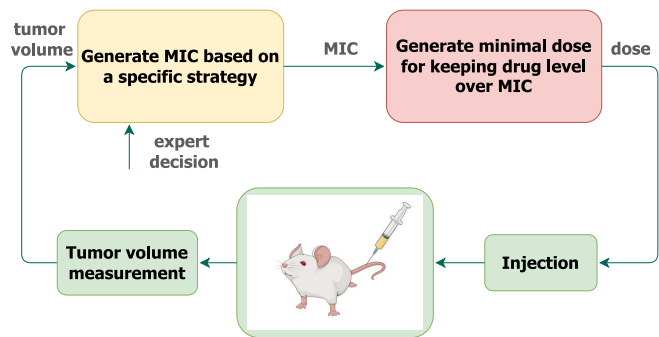

Fig. 1. Procedure of the therapy optimization: the MIC is specified based on a chosen strategy, and the minimal doses are calculated, which ensure that the drug level is over MIC.

version of the second one, which uses the minimal and maximal values of the parameters for a specific population and finds the minimal dosages to ensure that the tumor volume does not increase for the worst-case parameter combination (Section III-D). This strategy is based on interval arithmetics, briefly summarized in Section II-F. One can switch between the strategies based on the tumor response automatically, or the switching can be done manually by an expert (Fig. 1).

We carry out in vivo experiments with 29 mice with breast cancer (Section IV) and show with a log-rank test, that our algorithm significantly increases overall survival compared to a generic therapy.

II. METHODS

The mathematical methods used for the therapy optimization are based on the tumor model discussed in Section II-A. The pharmacodynamics of the model is detailed in Section II-B, which is needed to calculate the drug level that has to be maintained during the therapy. The required dosages are calculated based on the pharmacokinetics of the model discussed in Section II-C. Based on the pharmacokinetic model, the minimal dosages required to keep the drug level over a specified limit are calculated as a solution to an optimization problem discussed in Section II-D. In order to personalize the therapy, identification is carried out with a mixed effect model given in Section II-E. Interval arithmetics is reviewed in Section II-F, which will be used to design robust therapy when only the model parameter ranges are known.

A. Tumor Model

The therapy generation algorithm will be based on a fourth-order model describing tumor dynamics, pharmacodynamics, and pharmacokinetics [35], [36], defined by the equations

$$\dot{x}_1 = (a - n)x_1 - b\frac{x_1 x_3}{ED_{50} + x_3} \tag{1}$$

$$\dot{x}_2 = nx_1 + b\frac{x_1 x_3}{ED_{50} + x_3} - wx_2 \tag{2}$$

$$\dot{x}_3 = -(c + k_1)x_3 + k_2 x_4 \tag{3}$$

$$\dot{x}_4 = k_1 x_3 - k_2 x_4 \tag{4}$$

where x_1, x_2, x_3, and x_4 are the time functions of the living tumor volume, dead tumor volume, drug level in the central

This article has been accepted for inclusion in a future issue of this journal. Content is final as presented, with the exception of pagination.

KOVÁCS et al.: POSITIVE IMPULSIVE CONTROL OF TUMOR THERAPY—A CYBER-MEDICAL APPROACH
3

TABLE I
NOTATIONS, NAMES, AND DIMENSIONS OF THE PARAMETERS
OF THE TUMOR GROWTH MODEL

Parameter notation	Parameter name	Parameter dimension
a	tumor growth rate coefficient	day^{-1}
b	drug efficiency rate coefficient	day^{-1}
n	necrosis rate coefficient	day^{-1}
w	washout rate coefficient of dead tumor cells	day^{-1}
ED_{50}	median effective dose of the drug	$\text{mg} \cdot \text{kg}^{-1}$
c	clearance of the drug	day^{-1}
k_1	flow rate coefficient of the drug from the central to the peripheral compartment	day^{-1}
k_2	flow rate coefficient of the drug from the peripheral to the central compartment	day^{-1}

compartment (the blood), and drug level in the peripheral compartment (the tissues), respectively. The unit of the volumes is mm^3, while the drug levels are in $\text{mg} \cdot \text{kg}^{-1}$, compatible with the unit of the injected doses. The parameters of the model are positive and are listed in Table I.

The injections are considered as impulsive effects on the central compartment x_3, i.e., let the K number of injections take place at time instants $t_k \geq 0$, $k = 0, 1, 2, \ldots, K-1$ with $t_0 < t_1 < \cdots < t_{K-1}$ and injected doses $u_k \geq 0$, then there is a discontinuity of the first kind in x_3 at time t_k, such that

$$x_3\left(t_k^+\right) = x_3\left(t_k^-\right) + u_k. \tag{5}$$

The output of the system is the total tumor volume

$$y = x_1 + x_2 \tag{6}$$

since x_1 and x_2 cannot be measured separately in the experiments, only the total tumor volume, which is their sum.

B. Pharmacodynamic Model

The pharmacodynamics of the drug is defined by the Hill function $x_3(ED_{50} + x_3)^{-1}$ in (1) and (2), which is a common function used to model the effect of the drug [8], [40]. This function expresses that the effect of the drug is saturated, and after a given limit, increasing the drug level yields a very low increase in the drug effect. The median effective dose parameter ED_{50} is the drug concentration where the effect is 50%, i.e., the value of the Hill function is 0.5.

The desired value of the drug level in the central compartment that should be maintained by the therapy discussed in Section II-D depends on the value of ED_{50}. An important goal

of the therapy optimization will be to keep the drug level in the central compartment over the MIC.

One possible strategy, described in Section III-B, is to define the limit as a constant multiple of the ED_{50} parameter, i.e., MIC $= \kappa ED_{50}$. If κ is sufficiently large, the value of the Hill function is close to 1, i.e., close to the maximal effect of the drug. For example, for the value of $\kappa = 100$, the value of the Hill function is 0.99; thus, the drug has at least 99% effect during the therapy.

Another strategy is to calculate the MIC such that the drug prevents the tumor from growing with the lowest dosages during the therapy, which we discuss in Section III-C for personalized treatment, in the case of intrapatient variability for known model parameters, and as a worst-case treatment for a population to treat interpatient variability in Section III-D.

C. Pharmacokinetic Model

The pharmacokinetics of the model described by (3) and (4) is a linear time-invariant system. The input of the system is positive and impulsive and has an effect on x_3 as described by (5). Since the drug level in the central compartment (x_3) has a direct effect on the tumor as described by the term on the right-hand side of (1), the output y_p of the pharmacokinetic model is x_3. Thus, the state-space representation of the pharmacokinetic model is

$$\begin{pmatrix} \dot{x}_3 \\ \dot{x}_4 \end{pmatrix} = \underbrace{\begin{pmatrix} -c - k_1 & k_2 \\ k_1 & -k_2 \end{pmatrix}}_{A} \begin{pmatrix} x_3 \\ x_4 \end{pmatrix} + \begin{pmatrix} 1 \\ 0 \end{pmatrix} u \tag{7}$$

$$y_p = x_3 \tag{8}$$

with u being the sum of impulsive inputs that is written using Dirac-delta distributions δ [20], i.e.,

$$u(t) = \sum_{k=0}^{K-1} u_k \delta(t - t_k) \tag{9}$$

at $t \geq 0$, where K is the total number of injections, $t_k \geq 0$, $k = 0, 1, \ldots, K-1$ is the time of injections with doses $u_k \geq 0$, $k = 0, 1, \ldots, K-1$, and δ is the Dirac delta distribution, i.e.,

$$\delta(t) = 0, \quad \text{if } t \neq 0 \tag{10}$$

$$\int_{-\infty}^{\infty} \delta(\tau) d\tau = 1. \tag{11}$$

The output of the pharmacokinetic subsystem (7) produced from the impulsive inputs (9) at time t can be written as the sum of impulse responses w of the system as

$$y_p(t) = \sum_{k=0}^{K-1} w(t - t_k) u_k. \tag{12}$$

In order to avoid ambiguity, we note that from now on, we use the letter w to denote the impulse response of the pharmacokinetic subsystem (and not the washout rate from Table I, which we will not need in the remaining of this article). The impulse response of the pharmacokinetic subsystem at time $t \geq 0$ is

$$w(t) = \frac{\lambda_1 + k_2}{\lambda_1 - \lambda_2} e^{\lambda_1 t} + \frac{\lambda_2 + k_2}{\lambda_2 - \lambda_1} e^{\lambda_2 t} \tag{13}$$

where λ_1 and λ_2 are the eigenvalues of the system matrix A in (7) and can be expressed with the parameters as

$$\lambda_{1,2} = \frac{-(c + k_1 + k_2) \pm \sqrt{(c + k_1 + k_2)^2 - 4ck_2}}{2}. \quad (14)$$

The pharmacokinetic subsystem is kinetic, thus it is positive [41], [42], [43], [44], which implies that the impulse response of the system is also positive for all $t \geq 0$.

Theorem 1: The pharmacokinetic subsystem (7) is asymptotically stable and nonoscillatory [28].

D. Optimal Impulsive Therapy

One way to optimize impulsive therapy is to find the minimal injection doses in order to maintain a predefined drug level in the patient, i.e., look for the optimal injection doses u_k given at time instants t_k, $k = 0, 1, \ldots, K - 1$ such that $x_3(t) \geq$ MIC for all $t \geq 0$. This problem has been addressed by Kusuoka et al. [29], who formulated and solved this optimization problem for compartmental systems with a constraint that the input should also be positive.

Let $\boldsymbol{u} = (u_0, u_2, \ldots, u_{K-1})^\top$ and $\mathbf{1} = (1, 1, \ldots, 1)^\top$ be a column vector with elements of one and length K, and let $\boldsymbol{\Phi}$ be the matrix of impulse responses constructed as

$$\boldsymbol{\Phi} = \left\{ w(t_i - t_{j-1}) \right\}_{i,j} \quad (15)$$

where $i, j = 1, 2, \ldots, K$, and t_K is a time instant after the last injection, i.e., $t_K > t_{K-1}$. The purpose of t_K is to maintain the predefined drug level for a certain time after the last injection.

The goal is to have $y_p(t) \geq$ MIC for all $t \geq 0$, where MIC is the desired lower limit for the drug level, with the constraint that the injections are positive, and the goal of minimizing the total amount of injections. Since the pharmacokinetic subsystem is positive, asymptotically stable, and nonoscillatory, $y_p(t) \geq$ MIC for all $t \geq 0$ is equivalent to $y_p(t_k) \geq$ MIC for all t_k, $k = 0, 1, \ldots, K$. Thus, the optimization problem can be written as

$$\begin{aligned} \underset{u}{\text{minimize}} \quad & \mathbf{1}^\top \boldsymbol{u} \\ \text{subject to} \quad & \boldsymbol{\Phi} \boldsymbol{u} \geq \text{MIC} \cdot \mathbf{1} \\ & \boldsymbol{u} \geq 0. \end{aligned} \quad (16)$$

The solution to this optimization problem [29] is

$$\tilde{\boldsymbol{u}} = \text{MIC} \cdot \boldsymbol{\Phi}^{-1} \mathbf{1}. \quad (17)$$

This constrained optimization problem minimizes the sum of the drug dosages u (i.e., the cumulative dose) with the constraints such that the drug level in the central compartment is not less than the MIC at the time of the injections (before the drug is injected), and the drug dosages are non-negative.

E. Mixed-Effect Model

The application of the therapy generation algorithms requires the knowledge of the model parameters, i.e., prior parametric identification has to be carried out. If the modeled population has similar intrinsic and extrinsic parameters, then the mixed effect model is an efficient tool for parametric identification [45]. In brief, such models assume that actual

parameters for a subject—mouse—are random variates from a distribution characterized by their mean and variance (and typically assumed to be normal), and the focus of the estimation lies in these population parameters. These approaches capture the intraindividual correlations of repeated measured data and can be considered as a middle ground between estimating individual parameters and one global parameter set.

Individual variates are obtained similarly to residuals. In fact, a mixed model can be written (with a single level of grouping) as

$$\mathbf{y}_i = \mathbf{X}_i \boldsymbol{\beta} + \mathbf{Z}_i \mathbf{b}_i + \boldsymbol{\varepsilon}_i$$

where $\mathbf{y}_i$ is the response variable, $\mathbf{Z}_i$ describes the grouping structure, $\mathbf{b}_i$ represents the so-called random effects, while $\boldsymbol{\beta}$ is the vector of fixed effects, with $\mathbf{X}_i$ being the usual—fixed effects—design matrix, and $\boldsymbol{\varepsilon}_i$ being the usual error term. Typically, $\mathbf{b}_i \sim \mathcal{N}(\mathbf{0}, \boldsymbol{\Sigma})$ and $\boldsymbol{\varepsilon}_i \sim \mathcal{N}(\mathbf{0}, \sigma^2 \mathbf{I})$ is assumed [45]. In the present case, $\mathbf{y}_i$ means the measured tumor volumes, $\mathbf{X}_i$ and $\mathbf{Z}_i$ contain the times of the measurements, while $\boldsymbol{\beta}$ collects the parameters of the differential equations (with $\mathbf{b}_i$ being their associated random effects). The likelihood implied by the above model can be calculated, and maximum-likelihood estimation is readily possible (although often other variants are used).

A further complication in such parameter identification problems is that the model is specified through a system of differential equations from which no explicit formula can be derived for the response variable. The stochastic approximation expectation–maximization (SAEM) approach can be used, which is an extension of the classic EM algorithm [46], widely used to carry out maximum-likelihood estimation (locally) when the model depends on unobserved parameters, as described by Delyon et al. [47]. This is widely used to estimate models described by differential equations with mixed effects [48].

Calculations in the in vivo experiments given in Section IV of this study are carried out under R statistical environment version 4.1.0 [49] using the nlmixr package version 2.0.4 [50].

F. Interval Arithmetics

Interval arithmetics is an efficient tool to analyze expressions in which the variables are perturbed, but their lower and upper limits are known. We will use interval arithmetics in Section III-D to calculate the min–max therapy in the presence of parametric perturbations, i.e., calculate the minimal doses that ensure that the drug has inhibiting/killing effect all the time in the worst-case parameter combinations. We will use the notations and definitions from the work of Alefeld and Mayer [51].

Let $\underline{a}$ denote the lower limit of the variable a, and $\bar{a}$ denote the upper limit of the variable a, and let $[a]$ denote the closed interval of the possible values of a, i.e.,

$$[a] = [\underline{a}, \bar{a}]. \quad (18)$$

Let $\circ$ be a binary operation on intervals, such that $\circ \in \{+, -, \cdot, /\}$ defined as the set

$$[a] \circ [b] = \{a \circ b, a \in [a], b \in [b]\} \quad (19)$$

This article has been accepted for inclusion in a future issue of this journal. Content is final as presented, with the exception of pagination.

KOVÁCS et al.: POSITIVE IMPULSIVE CONTROL OF TUMOR THERAPY—A CYBER-MEDICAL APPROACH

5

where $0 \notin [b]$, if the operation is division. The results of the operations are the intervals

$$[a] + [b] = \left[\underline{a} + \underline{b}, \overline{a} + \overline{b}\right] \tag{20}$$

$$[a] - [b] = \left[\underline{a} - \overline{b}, \overline{a} - \underline{b}\right] \tag{21}$$

$$[a] \cdot [b] = \left[\min\{\underline{ab}, \underline{a}\overline{b}, \overline{a}\underline{b}, \overline{ab}\}\right]. \tag{22}$$

In the case if $\underline{a} > 0$ and $\underline{b} > 0$, we have that $[a] \cdot [b] = [\underline{ab}, \overline{ab}]$. The multiplicative inverse is defined as

$$\frac{1}{[b]} = \left\{\frac{1}{b} \middle| b \in [b] \right\}, \quad \text{if } 0 \notin [b] \tag{23}$$

which can be calculated as

$$\frac{1}{[b]} = \left[\overline{b}^{-1}, \underline{b}^{-1}\right]. \tag{24}$$

The standard interval functions are $\psi \in F = \{\sin, \cos, \tan, \arctan, \exp, \ln, \text{abs}, \text{sqrt}\}$, which are defined by their range as

$$\psi([x]) = \{\psi(x), x \in [x]\}. \tag{25}$$

Functions composed of standard interval functions and binary operations can be used in interval arithmetics based on the definitions.

If a function depends on an interval variable more than once, then we should use interval variables defined as the convex combination of their lower and upper limits [52], i.e.,

$$\tilde{a} = \alpha \underline{a} + (1 - \alpha)\overline{a}, \quad \alpha \in [0, 1]. \tag{26}$$

Let ψ be a function of a, then

$$[\psi] = \left[\underline{\psi}, \overline{\psi}\right] \tag{27}$$

with the lower limit defined as the solution of

$$\underline{\psi} = \min_{\alpha} \psi(\tilde{a}) \tag{28}$$

and the upper limit as the solution of

$$\overline{\psi} = \max_{\alpha} \psi(\tilde{a}) \tag{29}$$

with α constrained to the interval $[0, 1]$.

III. MAIN RESULTS

A. Tumor Dynamics

Consider the first two equations (1) and (2) of the tumor model and denote the drug effect by $E = bx_3(ED_{50} + x_3)^{-1}$. These equations describe the tumor dynamics

$$\dot{x}_1 = (a - n)x_1 - Ex_1 \tag{30}$$

$$\dot{x}_2 = nx_1 + Ex_1 - wx_2. \tag{31}$$

The equilibrium points of this model are the solutions to

$$0 = (a - n - E^*)x_1^* \tag{32}$$

$$0 = (n + E^*)x_1^* - wx_2^*. \tag{33}$$

The solutions are as follows.
1) $x_1^* = 0$ and $x_2^* = 0$.
2) $E^* = a - n$, and $x_2^* = (a/w)x_1^*$.

Steady-state 1 is the origin, which is ideally the goal of the therapy. Steady-state 2 is a nonzero equilibrium that is achieved if the drug effect and the tumor dynamics are balanced. Note that in steady-state 2, the variables can be zero, but in this case, we get steady-state 1.

The Jacobian of (30) and (31) is

$$\boldsymbol{J} = \begin{pmatrix} a - n - E^* & 0 \\ n + E^* & -w \end{pmatrix} \tag{34}$$

with the eigenvalues

$$\lambda_1 = a - n - E^* \tag{35}$$

$$\lambda_2 = -w. \tag{36}$$

Since the parameters are positive, we have that $\lambda_2 < 0$. In steady-state 2, we have $\lambda_1 = 0$, thus the steady-state is on the line $x_2^* = (a/w)x_1^* \neq 0$, if initially $x_1(0) > 0$. Steady-state 1 is asymptotically stable if $\lambda_1 < 0$, i.e., if $E^* > a - n$. Note that we are interested in the case when $a - n > 0$, i.e., the tumor grows without therapy.

Theorem 2: If $E(t) > a - n$ for all $t \geq 0$, then the origin of the model (30), (31) is asymptotically stable.

Proof: Let E_1 and E_2 be time functions that satisfy that $E_2 > E_1 > 0$, i.e., $E_2(t) > E_1(t) > 0$ for all $t \geq 0$, and let $x_1^{(1)}$ be the solution to (30) with input E_1 and $x_1^{(2)}$ be the solution with input E_2 to (30) with initial condition $x_1(0) > 0$. Due to the positivity of x_1 and E, we have that $\forall t \geq 0$

$$(a - n)x_1(t) - x_1(t)E_2(t) < (a - n)x_1(t) - x_1(t)E_1(t) \tag{37}$$

thus $x_1^{(1)}(t) > x_1^{(2)}(t)$ whenever $t > 0$. Thus, the tumor dynamics model is monotonous in E. Let $E_1 > a - n$ with $E_1 \equiv \text{const}$, and E_2 be an arbitrary function with $E_2(t) > E_1$ for all $t \geq 0$. Since $E_1 > a - n$, we have that $a - n - E_1 < 0$, thus the solution to (30) with initial condition $x_1(0)$

$$x_1^{(1)}(t) = e^{(a-n-E_1)t}x_1(0), \quad t \geq 0 \tag{38}$$

tends to zero; thus, the origin is asymptotically stable. Due to the monotonicity, $x_1^{(2)}(t) < x_1^{(1)}(t)$ for all $t > 0$, thus the solution with E_2 also converges to zero, since if $E_2 > E_1$, then

$$x_1^{(2)}(t) < e^{(a-n-E_1)t}x_1(0), \quad t \geq 0 \tag{39}$$

where the right-hand side tends to zero whenever $E_1 > a - n$. ∎

Thus, if the net effect E is kept over the limit $a - n$ during the whole therapy, then the total tumor volume tends to zero. For impulsive systems with linear pharmacokinetics and nonlinear pharmacodynamics, the effect of the drug can be kept over a specified limit with the method discussed in Section II-D. The following section will provide strategies to define this specific limit. In the original model $E = bx_3(ED_{50} + x_3)^{-1}$, thus we will provide limit for x_3 denoted as MIC.

Since the maximum of $x_3(ED_{50} + x_3)^{-1}$ is 1, the direct consequence of Theorem 2 follows.

Theorem 3: Suppose that $a - n > 0$. There exists x_3 such that the origin of the model (30), (31) is asymptotically stable if and only if $b > a - n$.

Proof: Suppose that $b > a - n$. In the original model, we use

$$E(t) = b\frac{x_3(t)}{ED_{50} + x_3(t)}. \tag{40}$$

Thus, in the applied tumor model, the effect E is in the interval $[0, b)$, provided that x_3 is always positive. Since

$$\lim_{x_3 \to \infty} b \frac{x_3}{ED_{50} + x_3} = b \tag{41}$$

we can always find a function x_3 which satisfies Theorem 2.

Now, suppose that the origin of the model is asymptotically stable. We show indirectly that it implies $b > a - n$. Suppose that $b < a - n$, and the origin is asymptotically stable. Thus, we have the limits

$$\lim_{x_3 \to \infty} \dot{x}_1 = \lim_{x_3 \to \infty} \left(a - n - b \frac{x_3}{ED50 + x_3} \right) x_1$$
$$= \underbrace{(a - n - b)}_{>0} x_1 \tag{42}$$

$$\lim_{x_3 \to 0} \dot{x}_1 = \lim_{x_3 \to 0} \left(a - n - b \frac{x_3}{ED50 + x_3} \right) x_1$$
$$= (a - n) x_1. \tag{43}$$

Since the function $x_3(ED_{50} + x_3)^{-1}$ is strictly monotonously increasing and $a - n - b < a - n$ due to the positivity of the parameters, the x_1 solution to (1) with initial condition $x_1(0)$ is bounded as

$$e^{(a-n-b)t} x_1(0) \leq x_1(t) \leq e^{(a-n)t} x_1(0) \tag{44}$$

where $e^{(a-n-b)t}$ tends to infinity due to (42); thus, the origin is unstable, which leads to a contradiction. ■

Due to the nonlinearity of E, the fourth-order model described by (1)–(4) can have rich dynamics; it was shown in [53], that if the therapy is considered to be continuous, i.e., we add u to the state x_3, and the applied control method is P-type control based on the total tumor volume $x_1 + x_2$, which is

$$u = -k(x_1 + x_2) \tag{45}$$

then the closed-loop system has a nontrivial equilibrium, and the system can have bifurcations with realistic parameter values. Moreover, the qualitative property of the equilibrium is independent of k.

B. Personalized Therapy With Maximal Effect

The critical parameter of the therapy design is the minimal drug level (denoted by MIC) that has to be maintained. If the MIC is known, the algorithm discussed in Section II-D only requires the knowledge of the pharmacokinetic parameters, and can be used to calculate the minimal doses. The value of MIC can be acquired intuitively or based on the pharmacodynamic parameters. For example, choosing MIC $= \kappa ED_{50}$ with κ sufficiently large ensures high efficiency for the therapy. The choice of $\kappa = 100$ results in 99% efficiency based on the pharmacodynamic model.

The advantage of the maximal effect is that it is robust against parametric perturbations due to oversized doses. The other advantage is that we only need to know the pharmacokinetic (PK) and pharmacodynamic (PD) parameters and do not require knowledge about the other tumor model parameters. Thus, the method can also be applied to other tumor models with similar PK and PD models. The disadvantage of the

method is the high level of toxicity that may result from the large doses. In order to avoid toxicity, the application of lower doses that still have inhibiting/killing effect may be desirable.

C. Personalized Therapy With Minimal Drug Level

One can also calculate MIC as the minimal drug level that ensures that the tumor volume does not increase between injections. This can be calculated in a personalized fashion if the model parameters of the patient are known. After the MIC is acquired, the algorithm defined in Section III-C is used to generate the required doses.

Theorem 4: The therapy ensures that the tumor does not grow using minimal doses if the drug level is kept over MIC $= \kappa ED_{50}$, where

$$\kappa \geq \frac{a - n}{b + n - a}. \tag{46}$$

Proof: The drug level ensuring that the tumor does not grow can be calculated based on (1), by considering that with the optimized therapy $x_3(t) \geq$ MIC for all $t \geq 0$, thus the net growth rate is

$$a - n - b \frac{x_3(t)}{ED_{50} + x_3(t)} \leq a - n - b \frac{\text{MIC}}{ED_{50} + \text{MIC}} \tag{47}$$

which implies that if we ensure that the net growth rate is smaller or equal to zero at the time of the next injection (prior to the injection), then the net growth rate is smaller than zero between the injections since the PK model is asymptotically stable without oscillatory behavior by Theorem 1 [29]. Thus, the tumor volume does not increase if we have

$$a - n - b \frac{\text{MIC}}{ED_{50} + \text{MIC}} \leq 0. \tag{48}$$

From this equation, we can express

$$\text{MIC} \geq \frac{ED_{50}}{\dfrac{b}{a - n} - 1} \tag{49}$$

and calculate the minimum value of κ by dividing the right-hand side with ED_{50}. ■

This result can be used to generate the minimal dose therapy that ensures that the tumor does not grow during the therapy. However, this approach only works if the parameters do not change during the therapy.

Now consider the case of intrapatient variability of the parameters, i.e., when the tumor model parameters change during the therapy. Suppose that the parameters are constant between injections and can only change at the time of injections. Let a^i, n^i, b^i, and ED_{50}^i denote the value of the parameters a, n, b, and ED_{50} prior to the ith injection with $i = 0, 1, \ldots, K - 1$, respectively. Let w^i denote the impulse response function of the PK model with the PK model parameter values prior to the ith injection, and $x_3^i(0^-)$ be the drug level at the time of the ith injection, without the injected dose. Note that we will use $t = 0$ as the time of the ith injection.

Let d_i denote the dose of the ith injection and T_i denote the time between the ith injection and $(i+1)$th injection. The drug level in the central compartment at time T_i is composed of the drug level due to the ith injection with a value of $d_i w^i(T_i)$

and the drug level due to the previous injections, denoted by $\tilde{x}_3(T_i)$, which can be calculated as

$$\tilde{x}_3(T_i) = \sum_{j=0}^{i-1} d_j w^j \left(\sum_{k=j}^{i} T_k \right) \tag{50}$$

if $i > 0$, and $\tilde{x}_3(T_0) = 0$. Thus, the drug level in the central compartment at time T_i is

$$x_3(T_i) = d_i w^i(T_i) + \tilde{x}_3(T_i). \tag{51}$$

Theorem 5: The therapy ensures that the tumor does not grow with minimal doses in the case of changing parameters if the drug level is calculated as

$$d_i \geq \frac{(a^i - n^i)ED_{50}^i - \tilde{x}_3(T_i)}{w^i(T_i)(b^i + n^i - a^i)}. \tag{52}$$

Proof: Between the ith and $(i+1)$th injections, we have to ensure that the net growth rate is not positive, which can be ensured if we have

$$a^i - n^i - b^i \frac{x_3(T_i)}{ED_{50}^i + x_3(T_i)} \leq 0 \tag{53}$$

for all $i = 0, 1, \ldots, K - 1$. Substituting (51) yields

$$a^i - n^i - b^i \frac{d_i w^i(T_i) + \tilde{x}_3(T_i)}{ED_{50}^i + d_i w^i(T_i) + \tilde{x}_3(T_i)} \leq 0 \tag{54}$$

from which we can express d_i to get (52). ∎

D. Min–Max Therapy for Uncertain Parameters

In the case of unknown parametric perturbations, we provide the minimal drug level dosing described in Section III-C, considering the worst-case scenario of parameter changes. This way, the therapy can handle interpatient variabilities in a robust manner. Let $\underline{a}$, $\underline{b}$, $\underline{n}$, and $\underline{ED}_{50}$ be the lower limits, while $\bar{a}$, $\bar{b}$, $\bar{n}$, and $\overline{ED}_{50}$ be the upper limits of the parameters a, b, n, and ED_{50}, respectively. Let $\underline{c}$, $\underline{k}_1$, and $\underline{k}_2$ be the lower limits, while $\bar{c}$, $\bar{k}_1$, and $\bar{k}_2$ be the upper limits of the parameters c, k_1, and k_2, respectively. Let d_i denote the drug dose of the ith injection and T_i denote the time between the ith injection and $(i+1)$th injection.

The time evolution of the drug level is characterized by the impulse response of the PK system, which has to be analyzed with interval analysis to calculate the worst-case value of the impulse response at time T_i. Let this worst-case value be denoted by $\underline{w}(T_i)$, which is the lowest value considering all the parameter combinations. Since the variables appear more than one time in the expression (13), we must define the interval variables

$$\tilde{c} := \underline{c}\alpha_c + \bar{c}(1 - \alpha_c) \tag{55}$$
$$\tilde{k}_1 := \underline{k}_1 \alpha_{k_1} + \bar{k}_1(1 - \alpha_{k_1}) \tag{56}$$
$$\tilde{k}_2 := \underline{k}_2 \alpha_{k_2} + \bar{k}_2(1 - \alpha_{k_2}) \tag{57}$$

as the convex combinations of the lower and upper limits of the parameters, i.e., we have $\alpha_c, \alpha_{k_1}, \alpha_{k_2} \in [0, 1]$. Then, the first eigenvalue of the system matrix is

$$\tilde{\lambda}_1 = \frac{-(\tilde{c} + \tilde{k}_1 + \tilde{k}_2) + \sqrt{(\tilde{c} + \tilde{k}_1 + \tilde{k}_2)^2 - 4\tilde{c}\tilde{k}_2}}{2} \tag{58}$$

while the second eigenvalue is

$$\tilde{\lambda}_2 = \frac{-(\tilde{c} + \tilde{k}_1 + \tilde{k}_2) - \sqrt{(\tilde{c} + \tilde{k}_1 + \tilde{k}_2)^2 - 4\tilde{c}\tilde{k}_2}}{2} \tag{59}$$

and the impulse response in the new variables is

$$\tilde{w}(T_i) = \frac{\tilde{\lambda}_1 - \tilde{k}_2}{\tilde{\lambda}_1 - \tilde{\lambda}_2} e^{\tilde{\lambda}_1 T_i} + \frac{\tilde{\lambda}_2 - \tilde{k}_2}{\tilde{\lambda}_2 - \tilde{\lambda}_1} e^{\tilde{\lambda}_2 T_i}. \tag{60}$$

In the worst-case PK parameter combination, the drug depletes fast thus we need the $\underline{w}(T_i)$ lower limit for the impulse response at time T_i after the ith injection, which can be calculated by solving the minimization problem

$$\begin{aligned} \underset{\alpha_c, \alpha_{k_1}, \alpha_{k_2}}{\text{minimize}} \quad & \tilde{w}(T_i) \\ \text{subject to} \quad & \alpha_c, \alpha_{k_1}, \alpha_{k_2} \in [0, 1]. \end{aligned} \tag{61}$$

This problem can be solved using numerical optimization for systems with nonlinear PK equations as well by replacing the impulse response function with the solution of the nonlinear differential equations depending on the uncertain parameters.

The worst-case value of the drug level in the central compartment T_i time after the ith injection is

$$x_3(T_i) = d_i \underline{w}^i(T_i) + \tilde{x}_3(T_i) \tag{62}$$

with

$$\tilde{x}_3(T_i) = \sum_{j=0}^{i-1} d_j \underline{w}^j \left(\sum_{k=j}^{i} T_k \right). \tag{63}$$

Theorem 6: The tumor volume does not grow during the therapy for the worst-case parameter combination if the applied dose is

$$d_i \geq \frac{(\bar{a} - \underline{n})\overline{ED}_{50} - \tilde{x}_3(T_i)}{\underline{w}(T_i)(\underline{b} + \underline{n} - \bar{a})}. \tag{64}$$

Proof: In order to guarantee that the tumor does not grow between two injections, we must have

$$a - n - b \frac{x_3(T_i)}{ED_{50} + x_3(T_i)} \leq 0 \tag{65}$$

where we supposed that the current injection takes place at $t = 0$, and the next injection occurs at $t = T_i$. Then, the value of the left-hand side of (65) is in the interval

$$[a] - [n] - [b] \frac{[1, 1]}{[1, 1] + \dfrac{[ED50]}{[x_3(T_i)]}} \tag{66}$$

$$= [\underline{a}, \bar{a}] - [\underline{n}, \bar{n}] - [\underline{b}, \bar{b}] \frac{[1, 1]}{[1, 1] + \left[\dfrac{\underline{ED}_{50}}{x_3(T_i)}, \dfrac{\overline{ED}_{50}}{x_3(T_i)} \right]}$$

$$:= [\underline{\varphi}, \bar{\varphi}]. \tag{67}$$

The therapy ensures that the tumor does not grow in the worst case if

$$\bar{\varphi} \leq 0. \tag{68}$$

This article has been accepted for inclusion in a future issue of this journal. Content is final as presented, with the exception of pagination.

8

IEEE TRANSACTIONS ON SYSTEMS, MAN, AND CYBERNETICS: SYSTEMS

Application of interval arithmetics discussed in Section II-F yields that

$$\overline{\varphi} = \overline{a} - \underline{n} - \underline{b}\frac{x_3(T_i)}{\underline{x_3(T_i) + \overline{ED}_{50}}}. \tag{69}$$

Substituting (62) into (69) yields

$$\overline{\varphi} = \overline{a} - \underline{n} - \underline{b}\frac{d_i\underline{w}^i(T_i) + \underline{\tilde{x}}_3(T_i)}{d_i\underline{w}^i(T_i) + \underline{\tilde{x}}_3(T_i) + \overline{ED}_{50}}. \tag{70}$$

Rearranging this equation to d_i and combining it with the inequality (68) yields the result. ∎

IV. In Vivo Test of the Results

A. Experimental Setup

The results were tested on a clinically relevant, genetically engineered mouse model of breast cancer. In this model, Brca1, a DNA repair gene, and p53, a regulator of cell cycle and genome stability, were knocked out in breast epithelial cells. The resulting mammary tumors highly resemble the Brca1-linked, triple-negative, hereditary breast cancer in humans: the molecular, immunohistochemical, morphological, and genetic characteristics are almost indistinguishable from their human counterpart [54].

Moreover, these tumors respond to chemotherapy very similarly; initial treatment with doxorubicin, docetaxel, or cisplatin significantly reduces tumor size and induces remission. However, long-term therapy often fails due to the emergence of drug resistance [55]. Despite we showed that PLD increases relapse-free and overall survival by 6- and 3-fold, respectively, these tumors cannot be cured using conventional chemotherapy regimens [37]. Findings obtained by using this model are frequently translated to human cancer clinics due to their similarity to human breast cancer.

The ideal therapy is personalized therapy, which is tailored to the specific patient. This requires knowledge of the patient-specific model parameters. However, the identification of the parameters requires several measurements, which is a large drawback of the method. The measurements can be used to carry out the parametric identification using a mixed-effect model described in Section II-E. The acquired parameters can be used to design optimal therapy using the algorithm described in Section II-D.

There were 29 mice divided into three groups.

1) *Control group (C):* Eight mice were treated with a standard protocol.
2) *Group S1:* Eleven mice, received 4 mg·kg^{-1} drug when the tumor first reached 200 mm^3, then the therapy was generated using the methods in Section III after tumor relapse.
3) *Group S2:* Ten mice, received 6 mg·kg^{-1} drug when the tumor first reached 200 mm^3, then the therapy was generated using the methods in Section III after tumor relapse.

The control group (C) treated with the standard protocol received 6 mg·kg^{-1} PLD, when the tumor reached 200 mm^3 volume, and the injections were repeated every 10 days if the
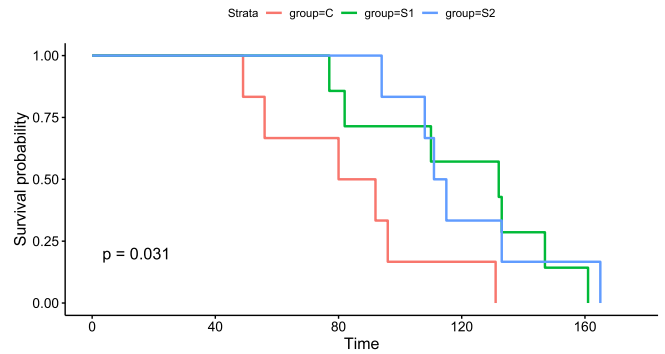

Fig. 2. Overall survival of the mice (in days). Time is calculated from the second injection, and the survival probability is calculated as the ratio of the living mice. The p value is the significance resulting from the log-rank test of the control group and the groups S1 and S2.

tumor volume was still over 200 mm^3. Otherwise, the treatment stopped until the tumor trigger, i.e., when the volume reached 200 mm^3 again. This protocol uses large doses (the maximal tolerable dose of PLD is 8 mg·kg^{-1}) with relatively large resting times (i.e., not less than ten days).

The mice in the experiments are genetically identical; thus, similar model parameters are expected. They were implanted tumor pieces derived from the same tumor, and their treatment started when their tumor first reached 200 mm^3. The tumor width and length were measured using calipers three times a week (on Monday, Wednesday, and Friday), and the tumor volume was approximated using the formula [33]

$$V = \frac{\pi}{3}(\text{width} \cdot \text{length})^{(2/3)}. \tag{71}$$

B. Results of the Experiment

The tumors reacted well to the first dose (4 mg·kg^{-1} in the case of group S1, and 6 mg·kg^{-1} in the case of group S2), and they shrank to a small volume (tumor remission). When the tumors started to grow back (tumor relapse) and reached 200 mm^3 again, we initiated a protocol based on our results presented here in groups S1 and S2. The mice received two injections per week, one on Tuesday and one on Friday. We set 6 mg·kg^{-1} as the maximal dose that can be given in one single injection.

At the time of the first relapse, we carried out parametric identification for the mice in groups S1 and S2 based on the previous measurements using the algorithm in Section II-E. We generated maximal effect therapies as given in Section III-B using $\kappa = 100$, i.e., the minimal drug level was 100 times the median effective dose, resulting in 99% effect of the drug.

We repeated the parametric identification on day 82 of the experiment. Based on expert knowledge, we changed the treatment strategy based on the following heuristics.

1) If the tumor volume was still over 200 mm^3, we continued applying the maximal effect therapy. If the resulting doses were larger than 6 mg·kg^{-1} with the new parameters, then we decreased the parameter κ to 10, i.e., the new minimal drug level was ten times the median effective dose, resulting in 90% efficiency.

This article has been accepted for inclusion in a future issue of this journal. Content is final as presented, with the exception of pagination.

KOVÁCS et al.: POSITIVE IMPULSIVE CONTROL OF TUMOR THERAPY—A CYBER-MEDICAL APPROACH 9
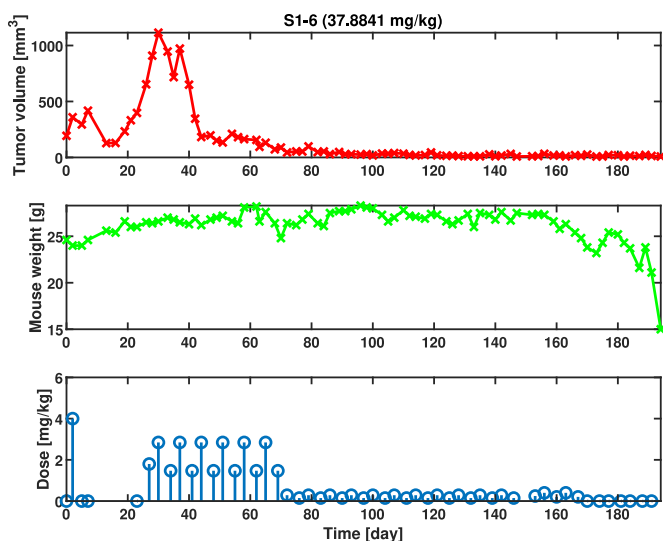

Fig. 3. Tumor volume measurements, weight measurements, and the injected doses for mouse 6 from group S1. The measurements are denoted with x-es, which are linearly interpolated for visualization.

Fig. 5. Tumor volume measurements, weight measurements, and the injected doses for mouse 1 from group C. The measurements are denoted with x-es, which are linearly interpolated for visualization.
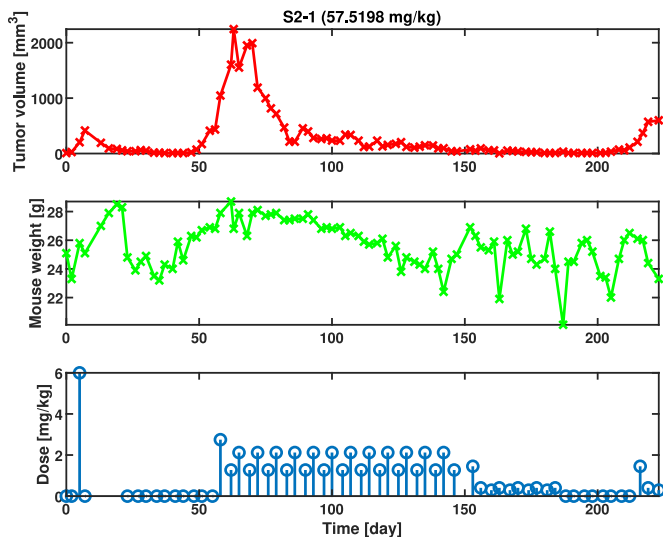

Fig. 4. Tumor volume measurements, weight measurements, and the injected doses for mouse 1 from group S2. The measurements are denoted with x-es, which are linearly interpolated for visualization.
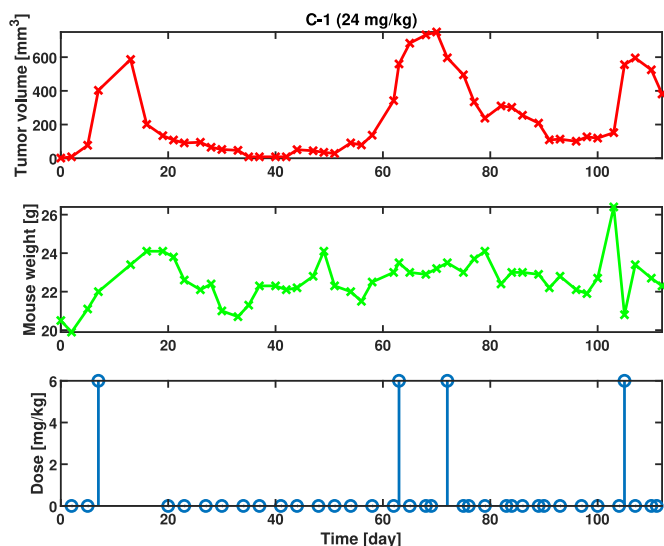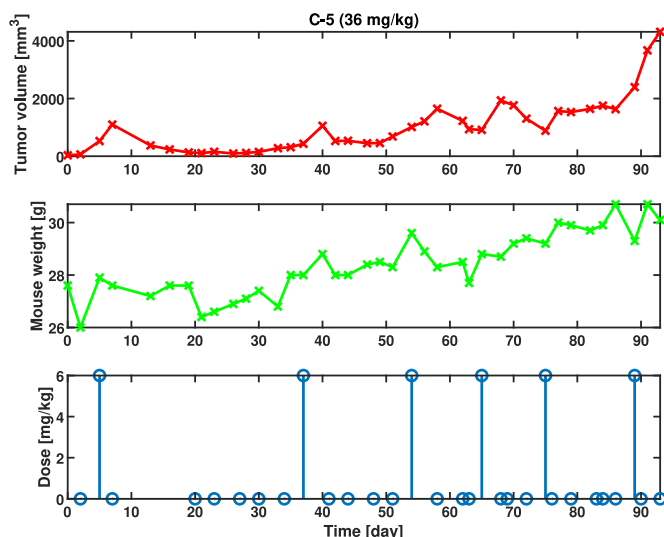

Fig. 6. Tumor volume measurements, weight measurements, and the injected doses for the mouse 5 from group C. The measurements are denoted with x-es, which are linearly interpolated for visualization.

2) If the tumor volume was under 200 mm^3, we switched to minimal drug level therapy described in Section III-C.

For comparison, we calculated the survival time of each specimen starting from the second injection since this is the time when the different treatment protocols started. The overall survival is shown in Fig. 2 for the three groups. The survival curves were estimated with the nonparametric method of Kaplan and Meier [56]. The equality of survival curves among different groups was tested with the nonparametric log-rank test [57], which resulted in a p-value of 0.031. This analysis showed that the strategies described in this article significantly increased the overall survival of the mice.

We show measurements for four selected mice in Figs. 3–6. The figures show the approximated tumor volumes, measured mouse weights, and injected doses. Two mice are selected from groups S1 and S2, and two from the control group C. Compared to the control group, the injections are more frequent in groups S1 and S2 and have smaller doses.

In these examples, the maximal tumor volumes were larger after relapse for the mice from groups S1 and S2, possibly due to the lower dosages of the drug. However, after the tumor remission, the tumor volume was kept at a low value with small dosages, while in the case of the control group, there were no injections after remission; thus, the tumor grew back after a short time. The results illustrate that the tumor can be kept at a low size with more frequent but smaller doses.

Based on these results, a suggestion for the application of the results is as follows.

1) Collect measurements.

2) Carry out parametric identification using the algorithm presented in Section II-E.

3) If the parameters of a specific patient are known, calculate the maximal effect therapy discussed in Section III-B. If toxicity is an issue, either decrease the effect by decreasing κ, or use the minimal dose therapy discussed in Section III-C.

4) If the patient-specific parameters are not known, but we have a priori measurements from a population with similar characteristics, we can use the ranges of the parameters to calculate the worst-case therapy discussed in Section III-D.

V. Conclusion

Cyber-medical systems in therapy generation may revolutionize the treatment of numerous diseases, including cancer. We proposed therapy generation algorithms based on a tumor model, supposing that the parameters of the model are known from an identification procedure.

The algorithms are based on an optimization that calculates the minimal injection doses, ensuring the drug level is kept over a specified limit based on personalized pharmacokinetic model parameters. We proposed strategies to determine this limit.

The maximal effect therapy is used to keep the drug level over a constant multiple of the median effective dose parameter to ensure that the drug has a predefined efficiency all the time. The advantage of this method is that it only requires extra knowledge of the pharmacodynamics, and by choosing a large multiplier, the robustness can be increased at the cost of toxicity.

We provide a formula for the minimal drug level that ensures that the tumor volume does not increase during the therapy. These results were generalized for the cases when intrapatient and interpatient variability of the parameters are present, providing a robust impulsive therapy solution.

The results were tested in in vivo experiments using 29 mice. The therapy generated with the proposed methods was compared to a generic protocol used in clinical practice. The superiority of our results was proved with a log-rank test, which showed a significant increase in overall survival.

The combination of the strategies given in Section III was carried out using heuristics in the experiments. This can be developed further by using feedback of the tumor volume, which can change the MIC after every sampling, or one can track the parameter changes and use the strategy in Section III-C to personalize the therapy and track intrapatient variability.

References

[1] E. Q. Wu, P. Xiong, Z.-R. Tang, G.-J. Li, A. Song, and L.-M. Zhu, "Detecting dynamic behavior of brain fatigue through 3-D-CNN-LSTM," *IEEE Trans. Syst., Man, Cybern., Syst.*, vol. 52, no. 1, pp. 90–100, Jan. 2022.

[2] W. Dang, Z. Gao, D. Lv, X. Sun, and C. Cheng, "Rhythm-dependent multilayer brain network for the detection of driving fatigue," *IEEE J. Biomed. Health Inform.*, vol. 25, no. 3, pp. 693–700, Mar. 2021.

[3] E. Q. Wu, C.-T. Lin, L.-M. Zhu, Z. R. Tang, Y.-W. Jie, and G.-R. Zhou, "Fatigue detection of pilots' brain through brains cognitive map and multilayer latent incremental learning model," *IEEE Trans. Cybern.*, vol. 52, no. 11, pp. 12302–12314, Nov. 2022.

[4] G. Kong, D.-L. Xu, J.-B. Yang, T. Wang, and B. Jiang, "Evidential reasoning rule-based decision support system for predicting ICU admission and in-hospital death of trauma," *IEEE Trans. Syst., Man, Cybern., Syst.*, vol. 51, no. 11, pp. 7131–7142, Nov. 2021.

[5] D. B. Larson, M. C. Chen, M. P. Lungren, S. S. Halabi, N. V. Stence, and C. P. Langlotz, "Performance of a deep-learning neural network model in assessing skeletal maturity on pediatric hand radiographs," *Radiology*, vol. 287, no. 1, pp. 313–322, 2018.

[6] S. Wang et al., "An ensemble-based densely-connected deep learning system for assessment of skeletal maturity," *IEEE Trans. Syst., Man, Cybern., Syst.*, vol. 52, no. 1, pp. 426–437, Jan. 2022.

[7] M. Gazda, M. Hireš, and P. Drotár, "Multiple-fine-tuned convolutional neural networks for Parkinson's disease diagnosis from offline handwriting," *IEEE Trans. Syst., Man, Cybern., Syst.*, vol. 52, no. 1, pp. 78–89, Jan. 2022.

[8] C.-M. Ionescu, "A computationally efficient hill curve adaptation strategy during continuous monitoring of dose-effect relation in anaesthesia," *Nonlinear Dyn.*, vol. 92, no. 3, pp. 843–852, 2018.

[9] P. H. Colmegna, R. S. Sánchez-Peña, R. Gondhalekar, E. Dassau, and F. J. Doyle, "Switched LPV glucose control in type 1 diabetes," *IEEE Trans. Biomed. Eng.*, vol. 63, no. 6, pp. 1192–1200, Jun. 2016.

[10] V. M. Pérez-García et al., "Computational design of improved standardized chemotherapy protocols for grade II oligodendrogliomas," *PLoS Comput. Biol.*, vol. 15, no. 7, 2019, Art. no. e1006778.

[11] T. Browder et al., "Antiangiogenic scheduling of chemotherapy improves efficacy against experimental drug-resistant cancer," *Cancer Res.*, vol. 60, pp. 1878–1886, Apr. 2000.

[12] L. Kovács et al., "Experimental closed-loop control of breast cancer in mice," *Complexity*, vol. 2022, pp. 1–10, May 2022. [Online]. Available: https://www.hindawi.com/journals/complexity/2017/5985031/

[13] I. Smalley et al., "Leveraging transcriptional dynamics to improve BRAF inhibitor responses in melanoma," *eBioMedicine*, vol. 48, pp. 178–190, Oct. 2019.

[14] A. R. Akhmetzhanov, J. W. Kim, R. Sullivan, R. A. Beckman, P. Tamayo, and C.-H. Yeang, "Modelling bistable tumour population dynamics to design effective treatment strategies," *J. Theor. Biol.*, vol. 474, pp. 88–102, Aug. 2019.

[15] J. M. Greene, J. L. Gevertz, and E. D. Sontag, "Mathematical approach to differentiate spontaneous and induced evolution to drug resistance during cancer treatment," *JCO Clin. Cancer Inform.*, vol. 3, pp. 1–20, Apr. 2019.

[16] D. A. Drexler, J. Sápi, and L. Kovács, "Optimal discrete time control of antiangiogenic tumor therapy," *IFAC-PapersOnLine*, vol. 50, no. 1, pp. 13504–13509, 2017.

[17] D. A. Drexler and L. Kovács, "Optimization of impulsive discrete-time tumor chemotherapy," in *Proc. IEEE 1st Int. Conf. Societal Autom.*, 2019, pp. 1–7.

[18] F. Cacace, V. Cusimano, and P. Palumbo, "Optimal impulsive control with application to antiangiogenic tumor therapy," *IEEE Trans. Control Syst. Technol.*, vol. 28, no. 1, pp. 106–117, Jan. 2020.

[19] H. Zhu, X. Li, and S. Song, "Input-to-state stability of nonlinear impulsive systems subjects to actuator saturation and external disturbance," *IEEE Trans. Cybern.*, vol. 53, no. 1, pp. 173–183, Jan. 2023.

[20] X. Li, H. Zhu, and S. Song, "Input-to-state stability of nonlinear systems using observer-based event-triggered impulsive control," *IEEE Trans. Syst., Man, Cybern., Syst.*, vol. 51, no. 11, pp. 6892–6900, Nov. 2021.

[21] E. Ahmadi, J. Zarei, and R. Razavi-Far, "Robust l_1-controller design for discrete-time positive T–S fuzzy systems using dual approach," *IEEE Trans. Syst., Man, Cybern., Syst.*, vol. 52, no. 2, pp. 706–715, Feb. 2022.

[22] S. Shi, Y. Chen, and X. Yao, "In vivo computing strategies for tumor Sensitization and targeting," *IEEE Trans. Cybern.*, vol. 52, no. 6, pp. 4970–4980, Jun. 2022.

[23] S. Shi, N. Sharifi, Y. Chen, and X. Yao, "Tension-relaxation in vivo computing principle for tumor sensitization and targeting," *IEEE Trans. Cybern.*, vol. 52, no. 9, pp. 9145–9156, Sep. 2022.

[24] S. Shi, Y. Chen, and X. Yao, "NGA-inspired nanorobots-assisted detection of multifocal cancer," *IEEE Trans. Cybern.*, vol. 52, no. 5, pp. 2787–2797, May 2022.

[25] H. Zhou and G. Alici, "A magnetically actuated novel robotic capsule for site-specific drug delivery inside the gastrointestinal tract," *IEEE Trans. Syst., Man, Cybern., Syst.*, vol. 52, no. 6, pp. 4010–4020, Jun. 2022.

[26] S.-M. Tse, Y. Liang, K.-S. Leung, K.-H. Lee, and T. S.-K. Mok, "A memetic algorithm for multiple-drug cancer chemotherapy schedule optimization," *IEEE Trans. Syst., Man, Cybern. B, Cybern.*, vol. 37, no. 1, pp. 84–91, Feb. 2007.

[27] P. Hahnfeldt, D. Panigrahy, J. Folkman, and L. Hlatky, "Tumor development under angiogenic signaling: A dynamical theory of Tumor growth, treatment response, and postvascular dormancy," *Cancer Res.*, vol. 59, no. 19, pp. 4770–4775, 1999.

[28] D. A. Drexler and L. Kovács, "Optimization of low dose metronomic therapy based on pharmacological parameters," *IFAC-PapersOnLine*, vol. 54, no. 15, pp. 221–226, 2021.

[29] H. Kusuoka et al., "Optimal control in compartmental systems and its application to drug administration," *Math. Biosci.*, vol. 53, nos. 1–2, pp. 59–77, 1981.

[30] J. S. Lowengrub et al., "Nonlinear modelling of cancer: Bridging the gap between cells and tumours," *Nonlinearity*, vol. 23, no. 1, pp. R1–R9, 2010.

[31] P. M. Altrock, L. L. Liu, and F. Michor, "The mathematics of cancer: Integrating quantitative models," *Nat. Rev. Cancer*, vol. 15, no. 12, pp. 730–745, 2015.

[32] A. M. Jarrett et al., "Mathematical models of tumor cell proliferation: A review of the literature," *Expert Rev. Anticancer Ther.*, vol. 18, no. 12, pp. 1271–1286, 2018.

[33] J. Sápi, L. Kovács, D. A. Drexler, P. Kocsis, D. Gajári, and Z. Sápi, "Tumor volume estimation and quasi-continuous administration for most effective bevacizumab therapy," *PLoS One*, vol. 10, no. 11, pp. 1–20, 2015.

[34] D. A. Drexler, J. Sápi, and L. Kovács, "Modeling of tumor growth incorporating the effects of necrosis and the effect of bevacizumab," *Complexity*, vol. 2017, Nov. 2017, Art. no. 5985031. [Online]. Available: https://www.hindawi.com/journals/complexity/2022/9348166/

[35] D. A. Drexler, T. Ferenci, A. Füredi, G. Szakács, and L. Kovács, "Experimental data-driven tumor modeling for chemotherapy," *IFAC-PapersOnLine*, vol. 53, no. 2, pp. 16245–16250, 2020.

[36] D. A. Drexler, T. Ferenci, A. Lovrics, and L. Kovács, "Tumor dynamics modeling based on formal reaction kinetics," *Acta Polytechnica Hungarica*, vol. 16, no. 10, pp. 31–44, 2019.

[37] A. Füredi et al., "Pegylated liposomal formulation of doxorubicin overcomes drug resistance in a genetically engineered mouse model of breast cancer," *J. Controlled Release*, vol. 261, pp. 287–296, 2017.

[38] J. G. Pierce and A. Schumitzky, "Optimal impulsive control of compartment models, I: Qualitative aspects," *J. Optim. Theory Appl.*, vol. 18, no. 4, pp. 537–554, Apr. 1976.

[39] M. Jacobs, "Optimisation of antimicrobial therapy using pharmacokinetic and pharmacodynamic parameters," *Clin. Microbiol. Infect.*, vol. 7, no. 11, pp. 589–596, 2001.

[40] B. Meibohm and H. Derendorf, "Basic concepts of pharmacokinetic/pharmacodynamic (PK/PD) modelling," *Int. J. Clin. Pharmacol. Therapeut.*, vol. 35, no. 10, pp. 401–413, 1997.

[41] A. I. Vol'Pert, "Differential equations on graphs (in Russian)," *Math. USSR-Sbornik*, vol. 17, no. 4, p. 571, 1972.

[42] P. Érdi and J. Tóth, *Mathematical Models of Chemical Reactions. Theory and Applications of Deterministic and Stochastic Models*. Princeton, NJ, USA: Princeton Univ. Press, 1989.

[43] J. Tóth, A. L. Nagy, and D. Papp, *Reaction Kinetics: Exercises, Programs and Theorems*. New York, NY, USA: Springer, 2018.

[44] D. A. Drexler, E. Virágh, and J. Tóth, "Controllability and reachability of reactions with temperature and inflow control," *Fuel*, vol. 211, pp. 906–911, Jan. 2018.

[45] J. C. Pinheiro and D. M. Bates, *Mixed-Effects Models in S and S-PLUS*. New York, NY, USA: Springer, 2000.

[46] A. P. Dempster, N. M. Laird, and D. B. Rubin, "Maximum likelihood from incomplete data via the EM algorithm," *J. Royal Stat. Soc. B, Methodol.*, vol. 39, no. 1, pp. 1–22, 1977.

[47] B. Delyon, M. Lavielle, and E. Moulines, "Convergence of a stochastic approximation version of the EM algorithm," *Ann. Stat.*, vol. 27, no. 1, pp. 94–128, 1999.

[48] S.-M. Chow, Z. Lu, A. Sherwood, and H. Zhu, "Fitting nonlinear ordinary differential equation models with random effects and unknown initial conditions using the stochastic approximation expectation–maximization (SAEM) algorithm," *Psychometrika*, vol. 81, no. 1, pp. 102–134, 2016.

[49] (R Foundation for Statistical Computing, Vienna, Austria). *R: A Language and Environment for Statistical Computing*. (2021). [Online]. Available: https://www.R-project.org/

[50] M. Fidler et al., "Nonlinear mixed-effects model development and simulation using nlmixr and related R open-source packages," *CPT Pharmacomet. Syst. Pharmacol.*, vol. 8, no. 9, pp. 621–633, Sep. 2019.

[51] G. Alefeld and G. Mayer, "Interval analysis: Theory and applications," *J. Comput. Appl. Math.*, vol. 121, no. 1, pp. 421–464, 2000.

[52] W. Lodwick (Univ. Colorado Denver, Denver, CO, USA). *Constrained Interval Arithmetic*. (1999). [Online]. Available: http://www-math.ucdenver.edu/ccm/reports/index.shtml

[53] D. A. Drexler, I. Nagy, and V. Romanovski, "Bifurcations in a closed-loop model of tumor growth control," in *Proc. 21th IEEE Int. Symp. Comput. Intell. Inform.*, 2021, pp. 329–334.

[54] X. Liu et al., "Somatic loss of BRCA1 and P53 in mice induces mammary tumors with features of human BRCA1-mutated basal-like breast cancer," *Proc. Nat. Acad. Sci.*, vol. 104, no. 29, pp. 12111–12116, 2007.

[55] S. Rottenberg et al., "Selective induction of chemotherapy resistance of mammary tumors in a conditional mouse model for hereditary breast cancer," *Proc. Nat. Acad. Sci.*, vol. 104, no. 29, pp. 12117–12122, 2007.

[56] E. L. Kaplan and P. Meier, "Nonparametric estimation from incomplete observations," *J. Amer. Stat. Assoc.*, vol. 53, no. 282, pp. 457–481, 1958.

[57] R. Peto and J. Peto, "Asymptotically efficient rank invariant test procedures," *J. Royal Stat. Soc. A, Gen.*, vol. 135, no. 2, pp. 185–207, 1972.

Levente Kovács (Senior Member, IEEE) received the M.Sc. degree in electrical engineering from the "Politehnica" University of Timişoara, Timişoara, Romania, in 2000, and the M.Sc. degree in biomedical engineering and the Ph.D. degree in electrical engineering from the Budapest University of Technology and Economics, Budapest, Hungary, in 2011 and 2008, respectively.

He is the Rector/President of Óbuda University, Budapest. He is a Full Professor with the John von Neumann Faculty of Informatics, Óbuda University, where he defended his habilitation with merit in 2013. He founded the Physiological Controls Research Center, Óbuda University in 2013, where he is the Deputy Head. He has published more than 500 articles in international journals and refereed international conference papers, accumulating an impact factor of over 120 and H-index of 30. His fields of interest are modern control theory and physiological controls.

Prof. Kovács was the President of IEEE Hungary Section from 2017 to 2020 and has been the President since 2022. In 2016, he founded the Cybernetics Technical Committee of the IEEE SMC Society, the Cyber-Medical Technical Committee, promoting the theory and practice of personalized healthcare.

Tamás Ferenci (Member, IEEE) received the Ph.D. degree in biostatistics from Óbuda University, Budapest, Hungary, in 2013.

He is with the Physiological Controls Research Center, Óbuda University. He is also with the Department of Statistics, Corvinus University of Budapest, Budapest, and the Department of Public Health, Semmelweis University, Budapest. He has published more than 90 journal papers. His current research interests include clinical biostatistics, epidemiology, and disease modeling.

Dr. Ferenci is an Editor of the *European Journal of Epidemiology*.

Balázs Gombos received the B.S. degree in biology from the University of Debrecen Clinical Center, Medical Microbiology, University of Debrecen, Debrecen, Hungary, in 2017, and the M.S. degree in molecular biology from the Faculty of Medicine, Department of Biochemistry and Molecular Biology, University of Debrecen in 2020. He is currently pursuing the Ph.D. degree in biology with the Drug Resistance Research Group, Research Centre for Natural Sciences, Budapest, Hungary, and with the Molecular Medicine Ph.D. School, Semmelweis University, Budapest, Hungary.

His current research interests include personalized chemotherapy and algorithm-assisted therapy design.

András Füredi received the M.Sc. degree in biophysics from the University of Szeged, Szeged, Hungary, in 2010, and the Ph.D. degree in molecular medicine from Semmelweis University, Budapest, Hungary, in 2018.

He is a Marie Curie Fellow with the Microsystems Laboratory, HUN-REN Centre for Energy Research, Budapest, while also a Project Leader with the Drug Resistance Research Group, HUN-REN Research Centre for Natural Sciences, and the Cybermedical Competence Center. He is also a Scientific Advisor for several Hungarian and international research and development companies. He is an expert in modeling human cancer in mice and developing novel drugs and treatment strategies to combat malignancies.

Imre Rudas (Life Fellow, IEEE) received the bachelor's degree in mechanical engineering from Don't Bànki Technical College, Budapest, Hungary, in 1971. He received the master's degree in mathematics from Eötvös Loránd University, Budapest, Hungary, in 1977, the Ph.D. degree in robotics and the Doctor of Science degree in computer science from the Hungarian Academy of Sciences, Budapest, in 1987 and 2004, respectively, and the Doctor Honoris Causa degrees in computer science from the Technical University of Košice, Košice, Slovakia, in 2001; the "Politehnica" University of Timişoara, Timişoara, Romania, in 2005; Óbuda University, Budapest, Hungary, in 2014; and the Slovak University of Technology in Bratislava, Bratislava, Slovakia, in 2016.

He is a Rudolf Kalman Distinguished Professor, a Rector Emeritus, and a Professor Emeritus with Óbuda University, Budapest. He has edited and/or published 22 books, published more than 890 papers in international scientific journals, conference proceedings, and book chapters, and received more than 8000 citations. His present areas of research activities are Computational Cybernetics, Cyber Physical Control, Robotics, and Systems of Systems.

Dr. Rudas was awarded by the Honorary Professor Title in 2013 and Ambassador Title by the Wrocław University of Science and Technology. He is the Junior Past President of the IEEE Systems, Man, and Cybernetics Society. He is a Fellow of the International Fuzzy Systems Association.

Gergely Szakács received the medical degree and Ph.D. degree in pathobiochemistry from Semmelweis University, Budapest, Hungary, in 1996 and 2001, respectively.

During his postdoc with National Cancer Institute (NIH), Bethesda, MD, USA, he discovered compounds targeting multidrug resistant (MDR) cancer, receiving two Federal Technology Transfer Awards. In 2005, he returned to Hungary to establish his lab with the support of the EMBO Young Investigator Program, a Marie Curie Fellowship, and grants from the Leukemia & Lymphoma Society and NIH. In 2012, he obtained an ERC Starting grant to support his research on innovative approaches to target MDR cancer. He has published several high-profile original papers and reviews on the "Achilles' heel" of multidrug resistant cancer. His research revolves around membrane transporters and drug resistant cancer. Based on his findings demonstrating the paradoxical sensitivity of cancer cells overexpressing the MDR exporter P-gp, he has aimed to exploit the collateral sensitivity of MDR cells.

Dr. Szakács received the Momentum Award established by the Hungarian Academy of Sciences with the aim to attract outstanding young scientists to Hungary in 2010. He is the Chair of the Excellence-Based Graduate Training Program (International Ph.D. Program for Translational Oncology) at the Medical University of Vienna.

Dániel András Drexler (Member, IEEE) received the Ph.D. degree in electrical engineering from the Budapest University of Technology and Economics, Budapest, Hungary, in 2015.

He is the Vice Deputy Head of the Physiological Controls Research Center, Óbuda University, Budapest, where he is also an Associate Professor with the John von Neumann Faculty of Informatics. He has published 119 papers in international scientific journals, conference proceedings, and book chapters and received over 1000 citations. His research interests include modeling and control of physiological, positive, and impulsive systems.

Dr. Drexler has been the Membership Development Officer of the IEEE Hungary Section since 2017 and the Vice Chair of the IEEE Hungary Section since 2021.